This is a repository copy of *Online damage detection of cutting tools using Dirichlet process mixture models*.

White Rose Research Online URL for this paper:
https://eprints.whiterose.ac.uk/190334/

Version: Published Version

Article:
Wickramarachchi, C.T. orcid.org/0000-0003-2454-6668, Rogers, T.J. orcid.org/0000-0002-3433-3247, McLeay, T.E. et al. (2 more authors) (2022) Online damage detection of cutting tools using Dirichlet process mixture models. Mechanical Systems and Signal Processing, 180. 109434. ISSN 0888-3270

https://doi.org/10.1016/j.ymssp.2022.109434

Reuse
This article is distributed under the terms of the Creative Commons Attribution (CC BY) licence. This licence allows you to distribute, remix, tweak, and build upon the work, even commercially, as long as you credit the authors for the original work. More information and the full terms of the licence here: https://creativecommons.org/licenses/

Takedown
If you consider content in White Rose Research Online to be in breach of UK law, please notify us by emailing eprints@whiterose.ac.uk including the URL of the record and the reason for the withdrawal request.

eprints@whiterose.ac.uk
https://eprints.whiterose.ac.uk/

Mechanical Systems and Signal Processing 180 (2022) 109434

Contents lists available at ScienceDirect

Mechanical Systems and Signal Processing

journal homepage: www.elsevier.com/locate/ymssp

Online damage detection of cutting tools using Dirichlet process mixture models☆

Chandula T. Wickramarachchi [a,b,*], Timothy J. Rogers [a], Thomas E. McLeay [c], Wayne Leahy [d], Elizabeth J. Cross [a]

[a] Dynamics Research Group, Department of Mechanical Engineering, University of Sheffield, Mappin Street, Sheffield S1 3JD, UK
[b] Industrial Doctorate Centre in Machining Science, Advanced Manufacturing Park, Wallis Way, Rotherham S60 5TZ, UK
[c] AB Sandvik Coromant, Mossvägen 10, 811 34 Sandviken, Sweden
[d] Element Six global Innovation Centre, Harwell Campus, Fermi Ave, Didcot OX11 0QR, UK

ARTICLE INFO

Communicated by J.E. Mottershead

Keywords:
Dirichlet process
Tool wear
PcBN
Unsupervised learning
Clustering
Damage detection

ABSTRACT

The ability to monitor and predict tool deterioration during machining is an important goal because the state of wear has a significant influence on the surface quality of machined components. To build up a comprehensive condition monitoring system for diagnosis and prognosis, however, extensive measurements and knowledge of tool wear is required. Collecting labelled datasets that include damage information for this purpose can be expensive and time consuming.

This paper suggests an unsupervised clustering approach using Dirichlet process mixture models to detect the change in characteristics of a cutting process online for diagnosis. As well as providing a useful monitoring tool, this approach has the potential to reduce the need for exhaustive wear measurements associated required for prognosis. The model is well suited to the erratic and unpredictable nature of tool wear progression, as the number of clusters required to determine the possible damage states are not set *a-priori*. Consequently, this method is equipped to handle variations across homogeneous and heterogeneous groups of tool material compositions.

The proposed approach is demonstrated here as a method to reduce the time required for trials for wear characterisation of new tools. In the example shown, the results indicate that the approach would result in around a 30% reduction of test times (on average) during outer diameter turning of case hardened steel, across 10 Polycrystalline cubic Boron Nitride tools from two different material compositions.

1. Introduction

Metal cutting or machining is the process in which material is removed in the form of swarf, to create a net shape through the relative movement between a tool and a workpiece [1]. One of the most significant yet unavoidable challenges in machining is the continuous wear on tools. Tool wear is the loss of material from the cutting surface due to interactions between the tool and the workpiece [2]. Tool wear is known to cause many issues to machined components, including form and dimension discrepancies,

☆ This work was part funded by EPSRC grant number EP/I01800X/1.

* Corresponding author at: Dynamics Research Group, Department of Mechanical Engineering, University of Sheffield, Mappin Street, Sheffield S1 3JD, UK.
E-mail addresses: c.t.wickramarachchi@sheffield.ac.uk (C.T. Wickramarachchi), tim.rogers@sheffield.ac.uk (T.J. Rogers), tom.mcleay@sandvik.com (T.E. McLeay), wayne.leahy@e6.com (W. Leahy), e.j.cross@sheffield.ac.uk (E.J. Cross).

https://doi.org/10.1016/j.ymssp.2022.109434
Received 6 April 2022; Accepted 8 June 2022
Available online 25 June 2022
0888-3270/© 2022 The Authors. Published by Elsevier Ltd. This is an open access article under the CC BY license (http://creativecommons.org/licenses/by/4.0/).

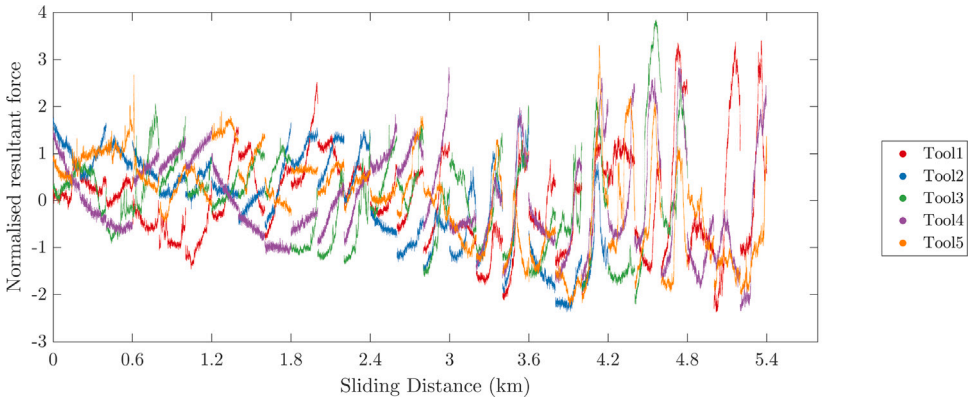

Fig. 1. The normalised resultant force collected from 5 PcBN tools under the same cutting conditions and workpiece materials. The sliding distance is the distance travelled by the tool. This data was collected using the same experimental test setup used in this paper (described in Section 3).

vibrations and chatter as well as insufficient surface finishes [3]. Machining with a worn or damaged tool will lead to surface defects on the component and crack propagation over time, resulting in non-acceptance or early retirement of that component. As a result, when machining safety critical components, industry employs a time-based maintenance strategy and discards tools at set times regardless of wear state. Typically, a tool could be retired with 50%–80% of useful life still remaining [4].

It is challenging to measure tool wear during machining owing to accessibility. However, by using indirect measurements of tool wear, such as acoustic emissions (AE), force and temperature, damage on the tool could be inferred without direct measurement [5–7]. With the help of machine learning techniques, this method may also be conducted in real time; tool condition monitoring (TCM) is an area of research dedicated to this topic.

TCM aims to move the industry focus from a preventative approach to a predictive maintenance strategy in order to reduce waste. Successful implementation of TCM systems are rarely found owing to the complex nature of machining, varying operating conditions and the availability of descriptive labels of wear states [8–13]. The variability between tools, and the high cost of extensive trials, unfortunately imply that supervised learning techniques for TCM are often not appropriate, as one must make the assumption that all tools wear in a similar manner to those used to establish or train a classifier [14]. The wear progression of tools can vary depending on inclusions and microstructure; properties that cannot be measured easily or predicted accurately due to their random nature. Take, for example, Fig. 1 that shows the normalised resultant force measurements from 5 turning tools (of the same material composition) under the same cutting conditions and workpiece materials, prior to failure. It is clear that the data from each tool behave dissimilarly to one another across tool life. As a result, the selection and classification of features that represent the damage across the entire tool set can be extremely challenging. Prognosis also requires damage labels (tool wear values) which are not only time consuming and expensive to collect, but introduces uncertainty to the data collection process. Furthermore, interesting, transient behaviours within the sensor data from continuous, indirect monitoring is often smoothed over in a prognosis setting; the data must be averages across time, between points at which damage labels are collected [15–17].

In the absence of an accurate TCM system, during the design and testing phase of a tool, leading designers such as Element Six. Ltd (E6) opt for off-line wear measurement in a run-to-failure method. This approach interrupts the cutting process intermittently and requires the temporary removal of the tool from the machine to complete wear measurements using optical microscopy. It is a time consuming and expensive method, that also introduces confounding influences[1] to the process such as positional differences, that in turn, could affect the cutting conditions and subsequently, the collected data and selected features.

The breakdown of time spent on a typical tool wear test setup at E6, is presented in Fig. 2. For reference, the same test setup is utilised in this paper. To improve the process efficiency, a TCM system should ideally aid the reduction of time spent on measurements to increase machining time.

It is the aim of this work to build a realistic TCM system using Dirichlet process mixture models (DPMMs), capable of dealing with confounding influences whilst retaining accuracy for inference over previously unseen tools (an unseen tool is usually either a new tool that has not been used for machining or a tool that has not been directly measured to obtain measurements of tool wear). The resulting system could, therefore, be more versatile than previous attempts [20,21] and may allow for easier implementation in industry.

Previous work on unsupervised learning of the machining process conducted by McLeay [21] focuses on using Gaussian mixture models (GMM) to cluster different damage and operational classes occurring on the tool. The author sets number of clusters *a-priori* for each tool by using the cluster information from the previous tool investigated. Because of the variance in tool behaviour as a result of confounding influences and the erratic nature of machining, it is challenging to classify wear states of unseen tools using this

[1] The features from a structure in its normal condition may show changes as a result of benign environmental or operation variations (or both), referred to as confounding influences [18]. Sometimes confounding influences can cause discontinuous changes in the features because of external operational influences [19].

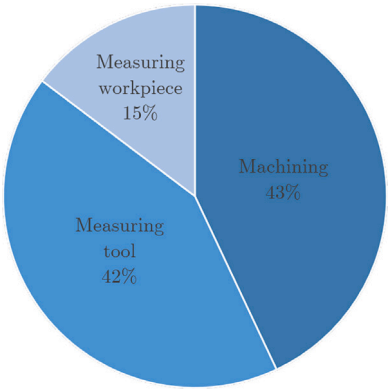

Fig. 2. The breakdown of time spent on a typical tool wear test setup at E6 that is explored in this paper.

technique. Similar studies on health assessment of composite structures [22,23] based on work in [24] has been conducted where the number of clusters were chosen *a-priori*. The initial results of [22] were found to be misleading owing to noise and the number of clusters were altered for accuracy. In [23] the number of clusters were optimised and damage state that correspond to the clusters were known. In [25] however, number of clusters were increased online using a Mahalanobis-like distance to measure similarity between clusters, although again, an in-depth understanding of the expected behaviour is required from supervised methods prior to testing. A similar methodology was undertaken in turbofan remaining useful life predictions where the clusters of unsupervised methods were used in a supervised way to inform the clusters of the testing phase [26]. These methods are unsuitable for the erratic nature of machining where variability in the data makes it challenging to choose the number of clusters prior to testing of unseen tools, even with a training phase.

DPMMs are used across numerous areas of research for clustering data. In the field of natural languages processing, the study of translation and text generation has led Vlachos et al. [27] to use DPMMs for clustering verbs. Dreyer et al. [28] applies the technique to organise and predict words. In medical research, DPMMs have been used to classify brain tissue from magnetic resonance imaging (MRI) scans [29]. Though GMMs perform effectively for well-defined tissue types, by not having to set number of clusters *a-priori* in DPMMs, the authors were able to classify abnormal brain data. In structural health monitoring (SHM), Rogers et al. [30] applied DPMMs to a three-storey building structure to successfully identify simulated damage. Furthermore, on the Z24 bridge dataset, DPMMs were able to detect damage whilst the structure was undergoing fluctuating environmental conditions.

The only previous use of DPMMs in the field of TCM was conducted by Liang et al. [31]. The authors computed the remaining useful life (RUL) of milling tools by supervised learning, using the DPMM. During the offline training stage, a wear model was built with force data generated by the tool alongside actual wear values, and the results were used to pick and weight the number of clusters of the DPMM. The learned model performed well and estimated conservative RUL for testing data. However, this work is not fully online and assumes that the tools used for testing performs similarly to the tools used for training, and also manually sets the number of clusters, meaning that this approach is as fallible as the supervised approaches mentioned earlier.

In this paper, DPMMs are used as an unsupervised method to detect characteristic changes in the data for online damage detection on a tool-by-tool basis. The authors apply DPMMs to an AE dataset, collected during a turning operation. The implementation of DPMMs here allows the assessment of tool condition to occur during machining without the need to collect any training data prior to the trial. There is also no need to select the number of possible clusters *a-priori*, alleviating the need for an in-depth prior knowledge of the machining process. The need for pre-labelled training data is also eliminated, reducing the costs associated with data collection.

This paper addresses the issues related to confounding influences introduced by fluctuating operations during trials by using two DPMMs in parallel. The intention here is that a new cluster initiation would be used to prompt an intervention, i.e., a manual inspection of the tool. As a result, the potential number of interruptions to the process is reduced. The aim is to increase the time spent on machining and reduce the time spent on tool measurement. By tracking the characteristics of the data through time, another goal would be to stop the machining process prior to failure, and reduce the number of early tool disposals. Although not covered in this paper (as it is beyond its scope), it may be possible to adopt a semi-supervised approach by adding damage labels to the model, reducing the number of false positives [30].

The structure of this paper is as follows. An introduction into DPMMs is given in Section 2 followed by the experimental setup in Section 3 then feature selection process in Section 4. The parallel DPMM is presented in Section 5 followed by promising results where clustering in the presence of confounding influences and clustering dissimilar tools within the subset are explored.

2. The Dirichlet process

An introduction to Dirichlet process Gaussian mixture models is given in this section where a Gaussian is used as the base distribution. A comprehensive explanation can be found in [30,32].

DPMMs can be used to cluster Gaussian and non-Gaussian data. The DPMM can be seen as an Infinite Gaussian Mixture Model (IGMM), where a mixture of Gaussian distributions are used to cluster the data. Here, the number of Gaussian distributions employed can tend to infinity, allowing the modelling of any non-Gaussian datasets; a cloud of data that does not follow a Gaussian distribution can be split into an infinite number of small clusters that are, themselves, Gaussian. IGMMs can also be used to learn information about the probability of each data point belonging to each cluster. The idea here is to find clusters within the data whilst also finding the parameters (size, shape) and the labels for those clusters. It is not possible to find the labels and the parameters of the clusters in one step, and so, Gibbs sampling is used in this work to infer the joint distribution. It is not a requirement for the DPMM to have knowledge of the number of clusters that may exist within the data before the algorithm is applied; the Gibbs sampler is able to initiate new clusters if data already evaluated by the algorithm is sufficiently different to the current data point.

The generative model of the DPMM is shown in Eqs. (1a)–(1e). In Gaussian mixture models, an assumption is made where each data point $\boldsymbol{x}_i$ ($i = 1, \dots, N$, N is the number of data points) is sampled from a Gaussian distribution (Eq. (1a)), a cluster of data with label c_i. For each Gaussian distribution, the conjugate prior is used (Normal Inverse-Wishart ($\mathcal{NIW}$) distribution over the mean (Eq. (1b)) and the covariance (Eq. (1c)) with hyperparameters, $\boldsymbol{\mu}_0$, $\Sigma_0, \kappa_0, \nu_0$) to achieve a closed form solution for the posterior. The data is normalised and the prior cluster has a zero mean and unit variance Gaussian in this work.

$$\boldsymbol{x}_i \mid c_i \sim \mathcal{N}(\boldsymbol{\mu}_{c_i}, \Sigma_{c_i}) \tag{1a}$$

$$\boldsymbol{\mu}_{c_i} \mid \Sigma_{c_i}, c_i \sim \mathcal{N}(\boldsymbol{\mu}_{c_i} \mid \boldsymbol{\mu}_0, \frac{\Sigma_{c_i}}{\kappa_0}) \tag{1b}$$

$$\Sigma_{c_i} \mid c_i \sim \mathcal{IW}(\Sigma_{c_i} \mid \Sigma_0, \nu_0) \tag{1c}$$

$$c_i \mid \boldsymbol{\pi} \sim \text{Mult}(\boldsymbol{\pi}) \tag{1d}$$

$$\boldsymbol{\pi} \sim \text{Dir}(\alpha) \tag{1e}$$

The cluster labels c are sampled from a multinomial distribution (Eq. (1d)). The mixing proportion, $\boldsymbol{\pi}$, is the probability of data belonging to each cluster. In order to calculate these probabilities, the Dirichlet distribution is used as it is the conjugate prior to the multinomial distribution (Eq. (1e)). $\boldsymbol{\pi}$ is controlled by the strength parameter α, the Dirichlet process prior.

Ultimately, the aim of this process is to find the posterior distribution over the cluster labels and the cluster parameters, from which the most likely label could be chosen. It is very difficult to find the probability of all cluster labels given all data, i.e.,

$$p(\boldsymbol{c} \mid \boldsymbol{X}) \tag{2}$$

as it is not possible to simultaneously infer the joint distribution over the labels and the cluster parameters ($\boldsymbol{\mu}_{c_i}$, Σ_{c_i}) whilst also finding the mixing proportion of all clusters.

The collapsed Gibbs sampler can be implemented to solve this. The collapsed Gibbs sampler sequentially samples new sets of cluster parameters based on samples of labels and new sets of labels based on parameters using

$$p(c_i \mid \boldsymbol{x}_i, X_{-i}, \boldsymbol{c}_{-i}). \tag{3}$$

Fig. 3 shows the steps followed by the Gibbs sampler. Each of these sampling steps can be done in closed form because of the selection of conjugate priors. In other words, it is a valid Markov chain Monte Carlo method that finds the distribution over the cluster labels and the distribution over the cluster parameters by alternating between the conditional posteriors. The collapsed Gibbs sampler is performed over a window of data, the length of which is specified according to available computation power.

Eq. (3) is the first probability distribution of interest. It is the probability that point $\boldsymbol{x}_i$ has the cluster label c_i given the model has seen all data X_{-i}, all other clusters $\boldsymbol{c}_{-i}$ and the new data point. This posterior probability has a multinomial distribution. Here, $-i$ means all the data points except for the data point i.

To compute this, the Gibbs sampler assigns the data randomly to clusters, and removed data points sequentially to update the cluster parameters and find the cluster best suited for that data point. The prior likelihood of drawing data from an existing cluster ($k = 1, \dots, K$) can be found in Eq. (4), where $N_{-i,k}$ is the number of data points in the current class and N is the total number of data points once the one being considered has been removed.

$$p(c_i = k \mid \boldsymbol{c}_{-i}, \alpha) = \frac{N_{-i,k}}{N + \alpha - 1} \tag{4}$$

The prior for a new cluster ($k^\star$) is calculated using

$$p(c_i = k^\star \mid \boldsymbol{c}_{-i}, \alpha) = \frac{\alpha}{N + \alpha - 1}. \tag{5}$$

The posterior predictive likelihood of the point belonging to each cluster should now be calculated, which is the probability of assigning the current data point to cluster k, given the value of the data, the current cluster the data is in, all the data already in that cluster and some hyperparameters.

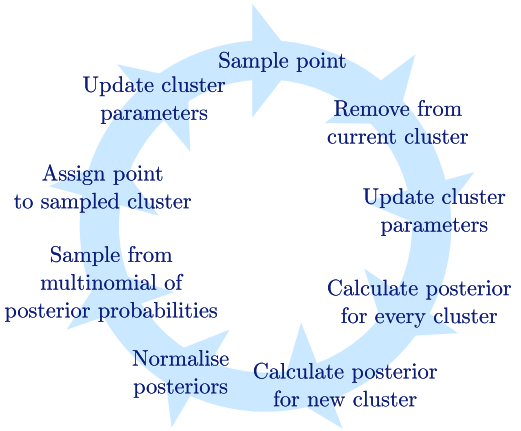

Fig. 3. The process of Gibbs sampling.
Source: Image reconstructed from [34].

To calculate the likelihood of the DPMM,

$$p(x \mid D_k) \tag{6}$$

is used, referred to as the posterior predictive distribution. This states the likelihood that the data point was generated by the cluster defined by the posterior distribution over the parameters, where D_k is all the data the algorithm has seen in a given cluster, k. For the DPMM model, this is represented by a Multivariate-T distribution which has heavier tails than a Gaussian, facilitating smaller clusters to accept new data points.

The posterior is normalised by the marginal likelihood, i.e. the sum of all the calculated posteriors to ensure it is a valid probability distribution, and to find the multinomial distribution for the cluster label c_i of point i. If the point is assigned to a new cluster, a $\mathcal{NIW}$ prior is used to initialise the cluster and the number of clusters are increased by one. This process is repeated until all the data in the window have been reassessed.

There are three main benefits of using this model. Firstly, it does not require an operator to set the number of clusters (or damage states in this case) before using the algorithm, which eliminates the need for prior knowledge of the process that can be impossible to obtain. Secondly, the whole model is controlled by the hyperparameters; hence threshold tuning, and calibration is not required. Thirdly, DPMMs permits the covariance function to change with the input data [33], resulting in a model that can handle dissimilar datasets which may be useful when detecting damage on multiple tools that wear differently to one another.

3. Experimental set-up

The test setup presented in Fig. 4(a) was used to collect data in order to explore the uses of DPMMs. This test setup is almost identical to the testing process at Element Six Ltd. (E6) (with the addition of AE sensors), where PcBN tools are used to dry machine (no coolant) case hardened workpieces[2] until catastrophic failure, i.e., where the cutting surface has broken, and the tool is no longer functional. These are referred to as 'end of life' tests. Often, coolant is not used when machining with PcBN owing to the material's susceptibility towards thermal shock. Subsequently, extremely harsh environments are generated in the machine, where swarf is known to get entangled around the workpiece during cutting.

The experiment was designed to test whether a successful implementation of a TCM method would be possible across different tool grades, to maximise the usefulness of the method in industry. As a result, data was collected from 10 tools of two different material compositions, or 'grades' of material; the grade of tool specifies the percentage of cubic boron nitride (cBN) particles within its composition. The grade has a direct effect on the behaviour of the tool and defines its suitability to a type of machining operation. The two grades used in this work are designed for continuous machining and are named Grade A (tools A1–A5) and Grade B (tools B1–B5) containing 55% and 45% cBN particles respectively. The standard cutting parameters and workpieces used at E6 for these tool grades were employed in this experiment in order to minimise the variability within the dataset. By doing so, the variability from altering the tool grades may be highlighted.

The typical run-to-failure method used at E6 – where tool measurements are taken every four passes of the workpiece[3] – was replicated in this work to explore where time and materials savings gains could be made. The tool inspections were also useful in determining whether the tool was still operational or has failed catastrophically. The inspection consists of removing the tool

[2] Case hardened workpieces (SAE8620) – used for automotive transmission components like gears or pinions – are used in this setup as it is a common application for PcBN. Case hardening is the process of rapidly heating and cooling a material to harden its outer surface.

[3] A pass consists of the tool removing the entire outer layer of the workpiece by moving from right to left in the z axis (Fig. 4(a)).

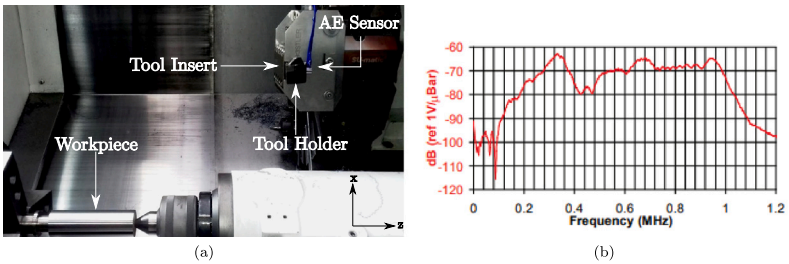

Fig. 4. (a) The set up of the machine and AE sensor. (b) The sensitivity of the AE sensor from [35].

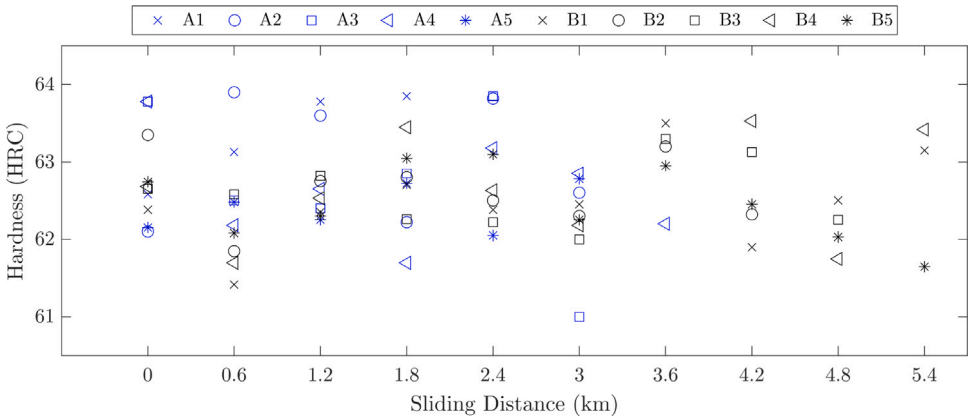

Fig. 5. The hardness of the workpieces at the start of each pass for all tools used in the experimental set-up. The hardness of the workpiece is a confounding influence as it has a significant affect on the chip formation mechanisms that in turn govern the AE signal characteristics.

from the machine to measure flank and crater wear using a 2D optical microscope and a 3D scanning microscope respectively. On average, it takes over 8 min to complete four passes and associated tool wear measurements. Over 42% of the time spent completing tool wear tests is spent on actions associated with these measurements.

In a review of around a decade's worth of research, Dornfeld et al. [36] discuss an enhanced sensitivity to tool wear when measuring acoustic emission (AE) compared to other common measurement types, on grounds that they are not hindered by low frequency disturbances. Here acoustic emissions were measured using a Mistras Micro-30D differential sensor with a sampling rate of 1 MHz (the sampling frequency was finalised via a feasibility trial [37] and previous literature [38–41]). The resonant frequency of the sensor was 125 kHz [35]. Fig. 4(b) presents the sensitivity of the sensor used in this work. The sampling rate results in a frequency range of 0–500 kHz when taking the Nyquist criteria into account. An Okuma Space Turn lathe LB3000 EXII was used for this experiment. In an attempt to gain further insight into the generating mechanisms for the AE, swarf was collected.

3.1. Confounding influences within the test setup

This setup has limitations and confounding influences that must be taken into consideration when choosing a model for TCM. Firstly, removing the tool for measurement is unavoidable as it is the only way to achieve a representative run-to-failure test set-up where damage labels are collected. When a tool is removed, it is not possible to secure it back to its exact position prior to measurement. As a result, the value of depth of cut (DOC) is uncertain for the next pass. DOC is pivotal to the mechanics of machining; varying the DOC can affect the forces, stresses, and dynamics of the process.

Secondly, workpieces are changed at every four passes of the workpiece introducing confounding influences to the setup and collected data. The workpiece change is necessary here because the case hardening (to around 62–64 HRC) only penetrates a small layer of the workpiece's outer diameter and is likely to be machined off after four passes. Therefore, at these four pass intervals, the workpiece is replaced by a new one. The largest operation variation (which is treated here as a confounding influence) is, therefore, the hardness of the workpieces. These were captured in the trial via hardness tests taken at the start (and end) of each pass. The hardness at the start of each pass for all tools are shown in Fig. 5 to demonstrate the variability of the workpiece properties.

4. Feature selection for the DPMM

In continuous turning, the tool is in constant contact with the workpiece, hence the generated AE takes the form of a continuous signal — an example of which is presented in Fig. 6. In this figure, the data is down sampled from around 1.9×10^9 to 5×10^6 datapoints

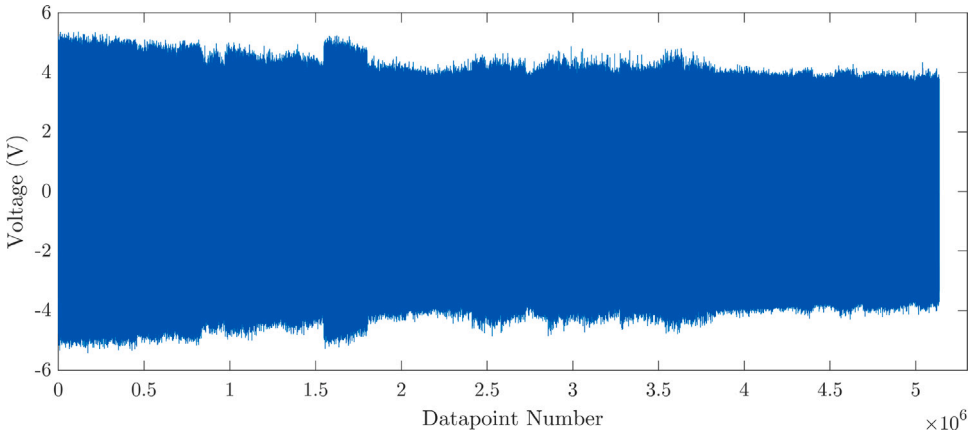

Fig. 6. A down-sampled time series of tool B3 to demonstrate the behaviour of AE in the time domain.

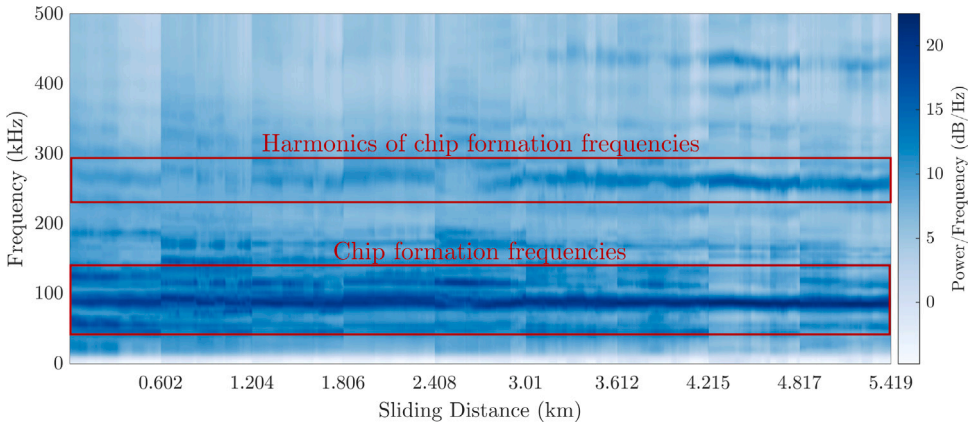

Fig. 7. The spectrogram of a PcBN tool at specific cutting conditions. The power of the signal is presented as the average power per unit bandwidth.

to demonstrate the general trends. The occurrences and sources of AE generation are numerous during continuous turning (and indeed in any machining), meaning that the traditional routes for AE analysis relying on separation of bursts are infeasible. AE signals from continuous turning are, therefore, challenging to analyse, and of course, have large storage requirements. One option for analysis is to consider summary statistics [42,43]. Here frequency domain features via spectrograms are utilised to allow the identification of informative continuous and transient features. Spectrograms also reduce the size of the dataset significantly, leading to faster computations when using machine learning algorithms.

In Fig. 7, a spectrogram for an example tool is displayed as a function of sliding distance, the distance travelled by the tool (as a constant cutting speed is used here, the sliding distance is equivalent to time). In order to transform the AE signals into the frequency domain using Short time Fourier transform, 50% overlapping Hamming windows with a length of 256 data points are used. In Fig. 7, the frequencies at which saw tooth formation on chips is assumed to be (also referred to as chip formation frequencies in this paper) are highlighted; as the machining process is conducted under dry conditions, i.e., coolant is not used, the main energy identified by the AE sensors is that of the plastic deformation of the workpiece material that produces the saw tooth on the chips. The harmonics of these frequencies are also highlighted; the harmonics occur possibly as a result of nonlinearities within the system, caused by plastic deformation and fatigue [44,45]. These harmonics do not correspond with sensor resonance.

Ultimately, DPMMs have the potential to be applied in an industrial setting to cluster data automatically when running online. From the spectrograms, the input features that are sensitive to tool degradation should have similar overall trends across a homogeneous[4] set of tools. The features can, however, include transient dissimilarities (from confounding influences such as change in workpiece, for example) because the DPMMs are flexible and, therefore, can account for these changes. From the spectrograms it is clear that the power of the harmonics of chip formation frequencies (equivalent to the root mean square of AE at the harmonic frequencies) increase in intensity with the progression of tool wear (Fig. 8). It is noted that the harmonics are relatively stable at

[4] In this case, homogeneous in the material composition and the nominally identical insert shape.

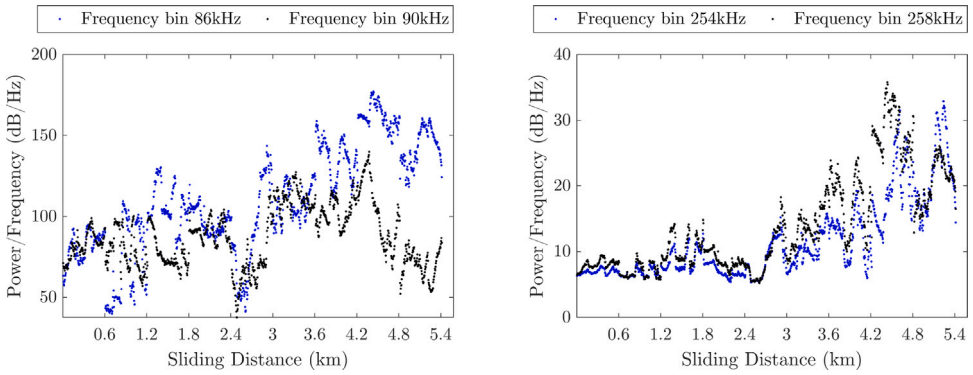

Fig. 8. The energy of the chip formation frequencies (left) and the first harmonics (right) from Fig. 7.

the start of tool life unlike the chip formation frequencies or the force measurements (as seen in Fig. 1), for example. Subsequently, four frequency bins (in 4 kHz intervals) that carry the harmonics of chip formation frequency (throughout the entire tool life) are standardised and chosen as candidate features for each tool grade.

It is important to note that prior knowledge of the process is required to identify these features that increase in intensity during the end of tool life. As the process is run online, it is not possible to identify this behaviour *a-priori* for a new tool. Here, the use of these frequency bands lessens the requirement on specific prior knowledge, however, identification of these bands is still necessary from preliminary trials for any new tool grade.

5. DPMMs in parallel

The clusters in DPMMs are formed due to change in mean and variance of the input features. In AE generation during machining, these changes of mean and variance are assumed to be caused by the onset of tool wear.

In the test set-up used in this paper, unavoidable confounding influences discussed in Section 3 such as the change in workpiece, or the positioning of the tool post measurement at the specified intervals, can also cause variations in the AE signal. It is important to differentiate between these two causes of cluster formation and tool wear when using DPMMs to avoid false positives.

In SHM, confounding influences [46] can present themselves as short and long term trends that must be distinguished from damage for accurate prediction. Cross et al. [47] approached this challenge by exploiting the cointegrated properties of time series. Amongst others, principal component analysis can also be used as a technique when dealing with confounding influences, where principal components with low variance can be used as features that are damage sensitive, yet unimpeded by prominent environmental trends [48]. Though these techniques are successful in suppressing unwanted trends, they require a set of representative training data *a-priori*.

In this work, a relatively simple solution is suggested for dealing with confounding influences whilst also retaining sensitivity to possible tool damage. It is proposed here to run two DPMMs in parallel:

1. The first DPMM is initiated at the start of each tool test and runs throughout tool life. This DPMM is referred to as the global DPMM henceforth.
2. The second DPMM is initiated at the start of each tool test and is reset at the start of each four passes of the workpiece, i.e. at the point where workpiece changes and tool positioning alterations occur. This DPMM will be named local DPMM.

The next section explores the application of the parallel DPMMs to the dataset described above.

5.1. Results

For each tool, the identified features are fed into two parallel DPMMs, where the Gibbs sampler is set with a window length of 200 (200 s of data from the chosen features), to enable the convergence to the target distribution.

Figs. 9 to 16 show the unsupervised clustering results for tools A1–A4 and B1–B4 from start to end of tool life. Each of these figures contain the results from the global DPMM on the left. On the right, the same four features clustered according to the local DPMM are presented. These figures are best viewed in colour.

For the global DPMM results, the clusters are presented in different colours, and the initiation of each cluster is demonstrated with a vertical line with the same colour as the cluster label, where the first cluster is initiated at the arrival of the first data point according to a threshold. The threshold value set here to be 1, specifies the number of data points a given cluster needs to have before it is identified as a new cluster. As this is an unsupervised method and does not require training on similar data, the DPMM is restarted from cluster 1 for each new tool. In the local DPMM results, the change of workpiece is indicated with dashed black

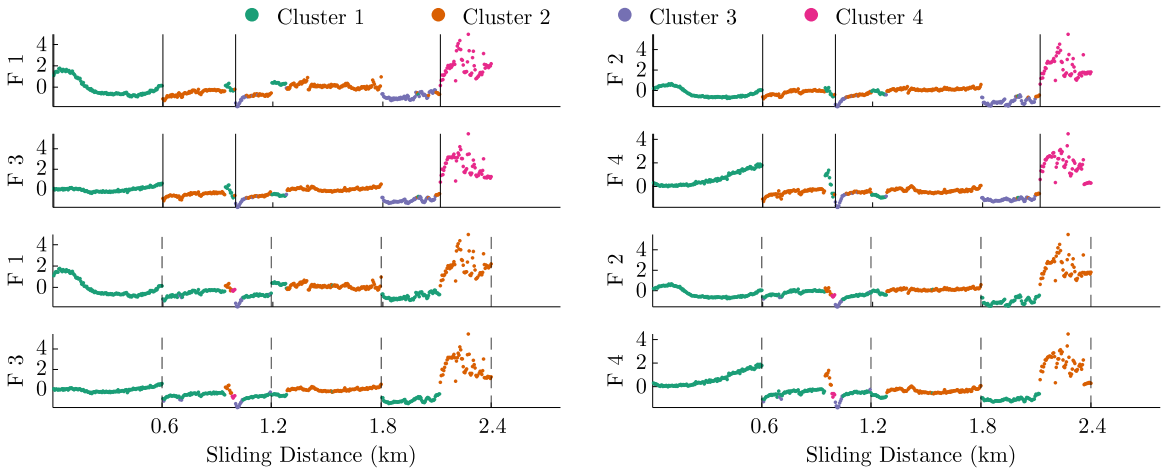

Fig. 9. DPMM clustering results for tool A1 using harmonics of the chip formation frequency from AE as input features. The top four plots show the global DPMM results and the bottom four plots represent the local DPMM results.

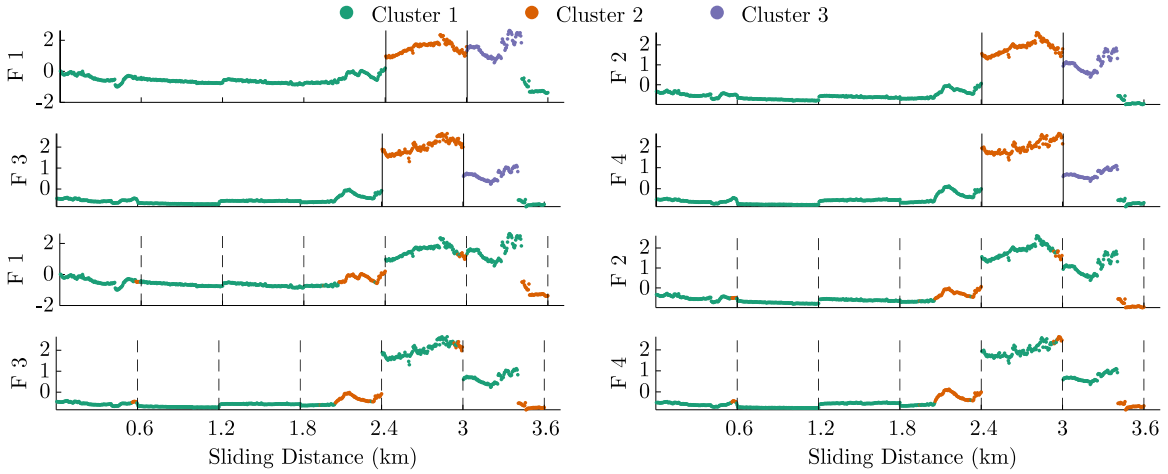

Fig. 10. The parallel DPMM clustering of tool A2.

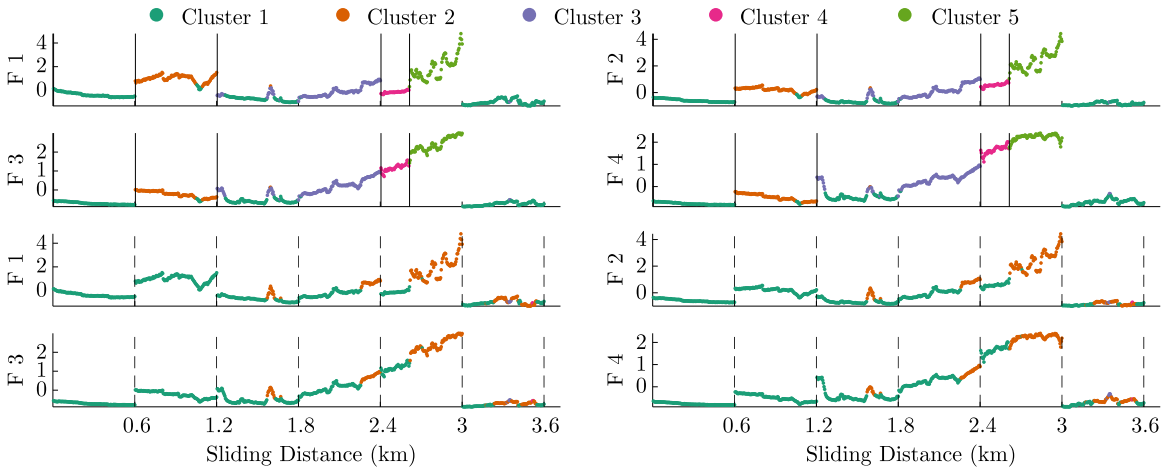

Fig. 11. The parallel DPMM clustering of tool A3.

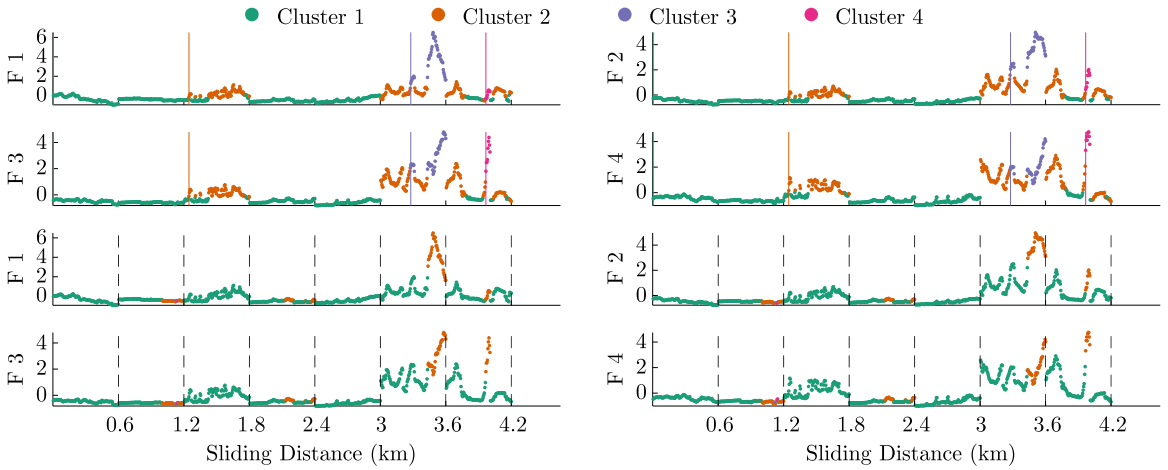

Fig. 12. The parallel DPMM clustering of tool A4.

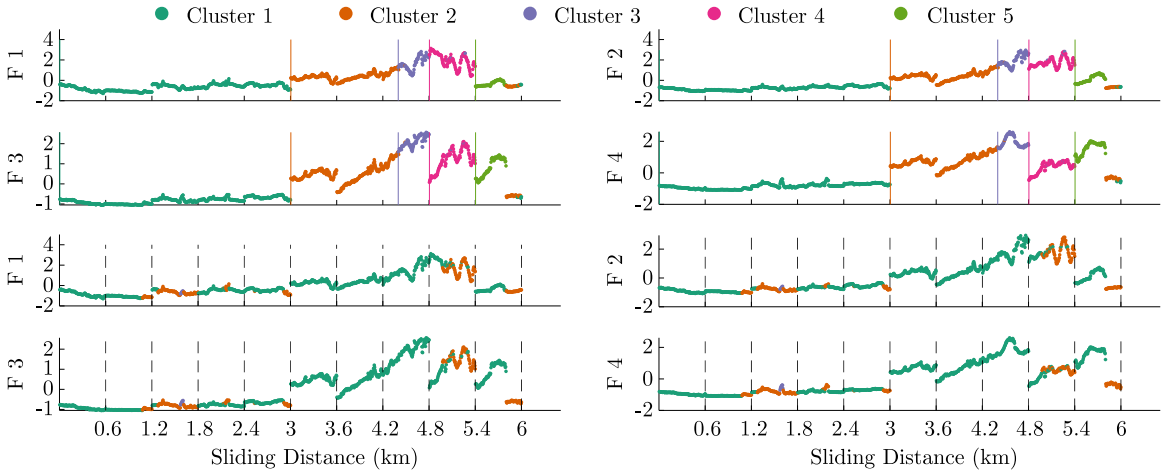

Fig. 13. The parallel DPMM clustering of tool B1.

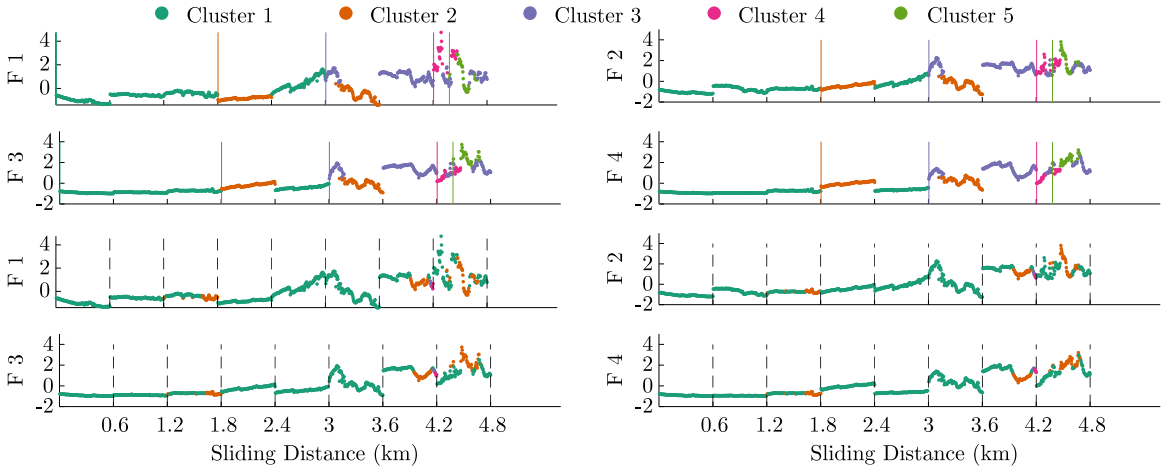

Fig. 14. The parallel DPMM clustering of tool B2.

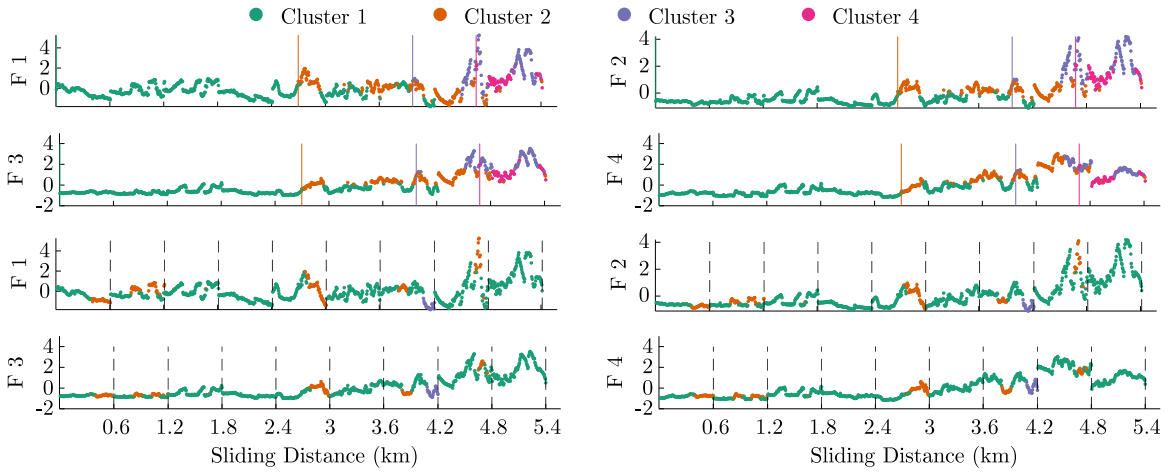

Fig. 15. The parallel DPMM clustering of tool B3.

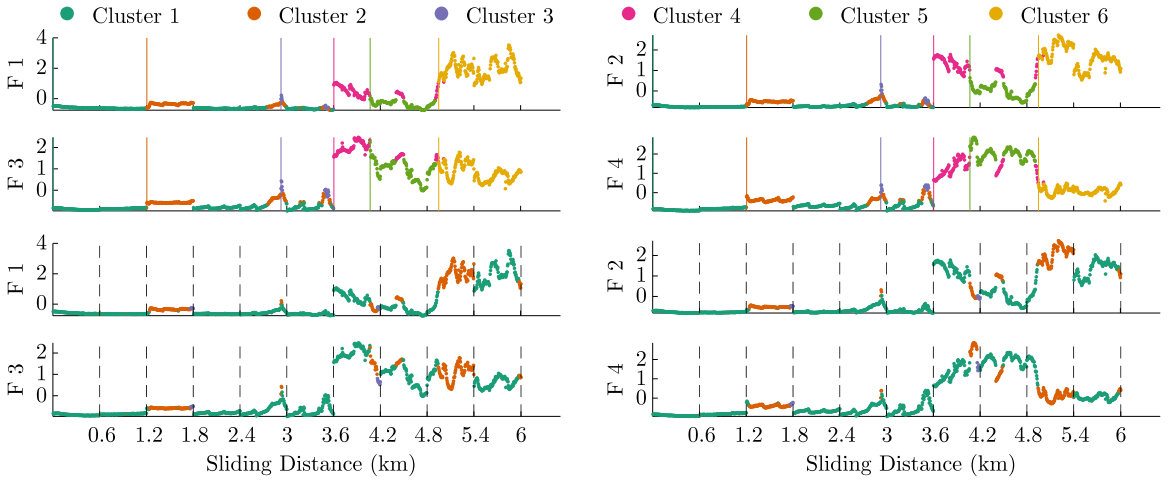

Fig. 16. The parallel DPMM clustering of tool B4.

vertical lines where the DPMM is reset to 1. The colour of the clusters are kept in the same order as the global DPMMs although the cluster initiation lines have not been shown for clarity.

In general, cluster 1 is usually the largest (discounting the effects of confounding influences), suggesting that the energy of AE harmonics does not vary enough to warrant a new cluster under the current hyperparameters. Physically, this could mean that the early wear progression of the tool does not significantly affect the harmonics of AE. In most cases, the energy of the harmonic frequencies increases rapidly near the end of tool life, due to tool wear. Owing to the large forces acting on the tool, small dislocations and micro cracks in the grain boundaries within the tool material release stress waves whilst also changing the wear profile of the tool. Consequently, the chip formation process may change permanently resulting in an increase in the energy of the AE signal. In the global DPMM, it is probable that these structural and conditional differences present themselves as non-Gaussian clusters, prompting the algorithm to separate into smaller Gaussians, leading to an increased number of clusters near the end of tool life.

Practically, the global cluster initiations could now be used as a warning of tool deterioration to the operator, where the appearance of a new cluster could be used to trigger an inspection rather than inspecting after a set sliding distance. The cluster initiations can, therefore, be considered as a novel method of setting a detection threshold. The observations from tool examination can be used to decide whether the tool is damaged beyond a pre-determined tolerance threshold or not. In the latter scenario, the new cluster can be treated as an undamaged state, thus allowing future classification of similar observations to the same cluster.

If, however, the cluster initiation occurs at the point of a workpiece change and tool measurement, the operator should refer to the local cluster initiations. In the case where the tool may be damaged at the start of the pass owing to the impact with the workpiece,

the local cluster is able to detect the corresponding variation in AE. In other words, the resetting of clusters at workpiece changes will essentially lead the local DPMM to only trigger new clusters when a significant change is seen in the data during machining of each workpiece. It can therefore be assumed that the changes are not due to anything other than tool wear (and associated effects such as increased temperature and force), as all the other operational influences are kept constant.

The results from hyperparameter investigation in the Appendix suggested that for this dataset, a small α value could be used as the clusters are well separated. This result is beneficial in the context of this work, as practically, cluster initiations are warnings for tool checks.

5.2. Other noteworthy observations

Some tools show that after initiations of new clusters, the data is sometimes grouped into a previous cluster. For example, after the third cluster initiation at around 4 km for tool B3 in Fig. 15, some data is still allocated to clusters 1 and 2. One explanation for this behaviour could be the changing cutting edge. As the tool traverses along the workpiece, it is constantly losing material from its cutting edge. It may be possible that some of the particles ejected from the tool are bigger than others, leading to a temporary hole in the cutting edge, causing the chip formation characteristics to change momentarily. As a result, the DPMM clusters the data into a new class. However, once the tool traverses along the workpiece after this event, it may be possible for the tool to smooth over the hole and return to an edge similar to earlier. At this point, the AE data would behave similar to the previous cluster, resulting in the behaviours seen in the figure. Without collecting high speed videos of the process, however, it is challenging to verify this assumption.

Another reason for the aforementioned clustering may be due to increased temperature at the cutting edge. In some cases, the produced chips can wrap themselves around the workpiece and gather at the cutting edge. In this case, the temperature at the cutting edge increases rapidly, burning the chips surrounding the tool. As a result, the chip formation characteristics may alter (and consequently, the generated AE) as the workpiece and tool temperatures affects the way the materials behave.

Although the return of the data to an earlier cluster may not be useful to an operator using the DPMM to monitor tools, this information can be useful for research and development purposes. This is especially true near the end of tool life where the data is clustered back to cluster 1 or 2 after tool failure, suggesting that the AE behave similarly to start of tool life. The reduced contact area between the tool and the workpiece may be a reason for this observation.

To avoid unnecessary inspections due to confounding influences, it is possible to increase the threshold value so that a larger number of data points are required before initiating a new cluster. However, the threshold value should be carefully considered as large values could mean that the cluster initiation is less sensitive to tool damage; the cluster will not be initiated until the threshold is met, in which time, the tool could be damaged catastrophically. An example of this can be seen in Fig. 16 where global cluster 2 is initiated, likely due to confounding influences: a change in workpiece. However, at this point, in the local DPMM, a second cluster is also immediately initiated suggesting that the data has been affected during the pass. This cluster initiation may be due to the tool's interaction with the workpiece as it comes into cut, where the sudden contact has affected the tool's chip formation characteristics. The initiation of cluster 4 is most likely due to confounding influences. Here, global clusters 3, 5 and 6 can be used as warnings to the operator to check for damage.

This method of parallel clustering is better suited to the tool damage detection problem than a two-class approach such as outlier analysis (otherwise known as anomaly detection) for a number of reasons. When conducting outlier analysis, the data are assumed to be sampled from Gaussian distributions in order for Gaussian statistics to apply. Any deviations from Gaussian distributions are seen as outliers indicative of abnormal data [49,50]. As discussed previously, the DPMM is able to separate larger non-Gaussian clusters into smaller Gaussians clusters automatically, without the need to set the number of clusters *a-priori*, and therefore detect abnormal data time and time again. By assigning data to multiple clusters, it is also possible to learn about the deterioration stages of the tool throughout time whilst also being robust against confounding influences. For example, the second cluster initiation of tools A2 and A3 and the fourth cluster initiation of tools B1 and B4 occur due to a large variation in AE energy compared to the previous data. From tool wear inspections, it is clear that these initiations were not caused by damage. By using the parallel DPMM method it should be possible to avoid operator intervention at these instances, whereas the same cannot be said for outlier analysis.

Given the lack of continuous wear measurements, it is difficult to directly validate that the DPMM is clustering at significant points. A means of partially assessing the success of the DPMM is in considering the trials where anomalies or irregularities were noted. In the next section, clustering of dissimilar tools are explored to investigate this further.

5.3. Results for tools that behave dissimilarly to others

In a supervised learning setting, prediction of tool wear states for a tool dissimilar in the dataset can lead to low accuracies (when the training set is not representative of the test set [45]). An advantage of the methodology presented here is that the analysis can be carried out on a tool-by-tool case, as there is no requirement for a training/characterisation phase. To demonstrate this, the results for tools used within the trial which were noted to exhibit behaviour that was dissimilar to other tools in that grade are presented here.

Figs. 17 and 18 show the results of the global and local DPMMs for tools A5 and B5 respectively. For comparison, the same features and hyperparameters are used for these tools as with all other tools within each grade. It is clear in both cases that the AE features behave differently to others in the dataset. It can be seen that the global DPMM detects cluster 3 at around 1.6 km and 3 km for tools A5 and B5 respectively, due to an unknown behaviour causing AE energy to rise at these specified frequencies. Due to

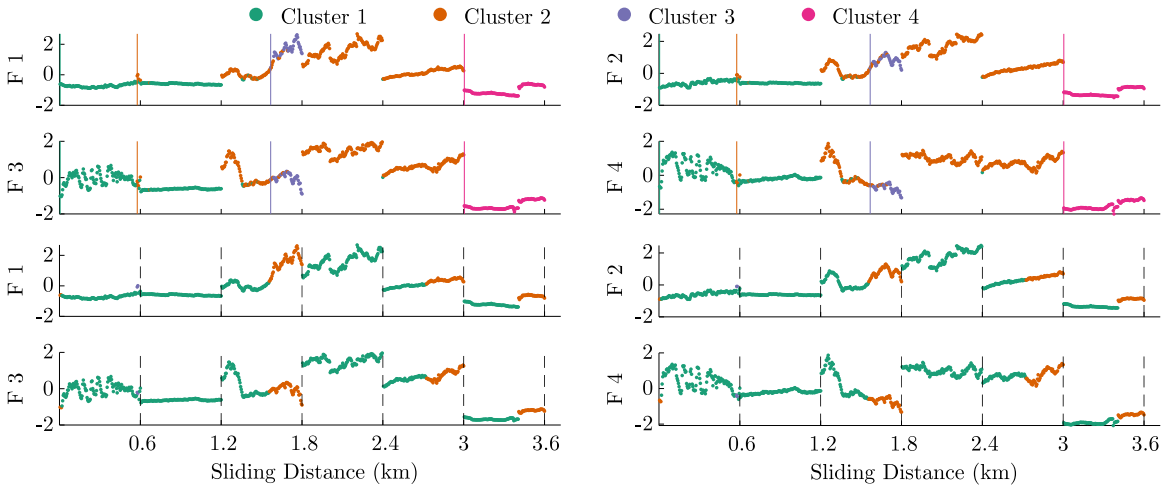

Fig. 17. The parallel DPMM clustering of dissimilarly behaving tool A5.

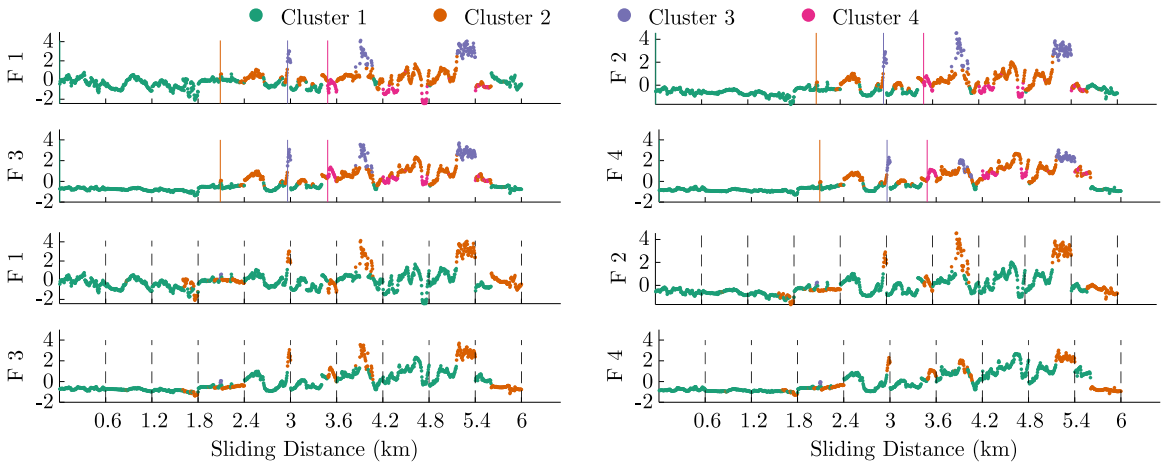

Fig. 18. The parallel DPMM clustering of dissimilarly behaving tool B5.

this increasing energy in the middle of tool life, the global DPMM does not detect a new cluster around 2.7 km (A5) and 5.2 km (B5) even though the energy of the signal has increased comparative to the start of tool life. At this point, however, the local clustering has created a second cluster to reflect this energy increase, that could be used for intervention and avoid machining with a broken tool. As the DPMM does not rely on data from other tools for training, it is able to cluster dissimilar data in a way that machining with a damaged tool may be avoided still. This suggests that the DPMM is robust against a large range of tool behaviours, and suggests its appropriateness and flexibility in this setting.

5.4. Guidelines for parallel DPMM to avoid tool failure

In order to correctly identify when a tool may be close to failure and to avoid false positives, guidelines for parallel DPMMs are suggested.

- The global clustering should take priority over local clustering, unless a global cluster has initialised at the point of a workpiece change. This is because the global clustering takes the entire dataset into account and as a result, it will be sensitive to large changes in the dataset. As the workpiece change can cause new clusters, the clusters at workpiece changes should be treated with caution.
- If a global cluster has been initiated at the point of a workpiece change, and a local cluster gets initiated during that workpiece, the initiation of that local cluster should be used as a warning.

Table 1
Summary of time savings when using DPMMs compared to other monitoring strategies. As the run-to-failure method leads to over 42% of test times on tool measurements, the DPMM leads to significant time savings.

Tool	Time spent on measurement (min)			% of time spent on measurement after applying DPMMs
	Run-to-failure tests	Preventative strategy	DPMMs	
A1	13.4	10.1	6.7	21.0
A2	20.2	16.8	3.4	7.0
A3	20.2	16.8	6.7	14.0
A4	23.5	20.2	6.7	12.0
B1	33.6	30.2	10.1	12.6
B2	26.9	23.5	3.4	5.3
B3	30.2	26.9	10.1	14.0
B4	33.6	30.2	13.4	16.8
Average	25.2	21.8	7.6	13.2

– If a global cluster has been initiated at the point of a workpiece change, but no local clusters are initiated during the workpiece, the global cluster initiation should be ignored as a warning.

5.5. Time savings through parallel DPMM

By running the DPMMs in parallel, it could be possible to reduce time spent on tool measurements whilst also avoiding machining with a broken tool. A complete list of time savings is presented in Table 1. In the table, the time spent on measurement using the DPMM is compared against a run-to-failure strategy (currently used in tool manufacturing environments) and a preventative maintenance strategy. In run-to-failure, the tool is measured after 4 passes of the workpiece and used until catastrophic failure. In the preventative strategy the operator stops machining when the tool meets a pre-defined threshold (decided according to the machining operation). In this paper, this threshold is assumed to be at the point of the last tool inspection prior to failure (for example, for tool B3 in Fig. 15 the last tool inspection is at a sliding distance of 4.8 km, resulting in 8 measurements totalling a measurement time of 26.9 min). Promising initial results show that tool measurement time could be reduced significantly from 42% to 13.2% of average test times when using this method.

Although these time savings are significant, it is important to note that future trials are needed at this point to validate that the cluster initiations are due to the posited change in wear characteristics. A step towards validation was taken by showing that the parallel DPMMs can be used to cluster data of dissimilar tools in order to avoid tool failure. Further experiments to obtain information about the chips at cluster initiations may be helpful in order to validate this model.

6. Conclusions

This paper explored the use of unsupervised data-driven learning to build a tool condition monitoring system for industry use, that can be implemented online without the need for a training dataset from new tools. To this end, a novel method that combined local and global Dirichlet Process mixture models (with Gibbs sampling) running in parallel were used to cluster AE data collected from a turning process on a tool-by-tool basis. Some of the main findings from this work were:

- By using unsupervised cluster initiations as warnings/prompts to the operator to conduct tool state investigations, the DPMM may be used successfully to reduce the time taken in tracking tool wear, particularly in a tool development setting, and provide a point at which tools can be retired.
- The method works successfully for tools of different material composition and tools that behave atypically in comparison to others.
- The DPMM running in parallel was able to account for the operational variations/confounding influences (from changing workpieces) that often affect the collection of tool wear related data.
- In the context of tool development and wear characterisation, initial results suggested that an intervention using this method would lead to a significant time reduction during trials (42% to 13.2% of average test times when using the DPMM).
- The number of clusters of the DPMM do not need to be set *a-priori*, leading to an entirely online implementation of the algorithm.
- The DPMMs avoided the need to gather extensive representative training data, or a training phase, and was able to detect changes in the monitored process with incomplete damage label sets.

CRediT authorship contribution statement

Chandula T. Wickramarachchi: Conceptualization, Methodology, Formal analysis, Investigation, Writing – original draft, Visualization. **Timothy J. Rogers:** Software, Writing – review & editing. **Thomas E. McLeay:** Supervision, Writing – review & editing, Resources. **Wayne Leahy:** Supervision, Writing – review & editing, Resources, Funding acquisition. **Elizabeth J. Cross:** Supervision, Writing – review & editing, Funding acquisition.

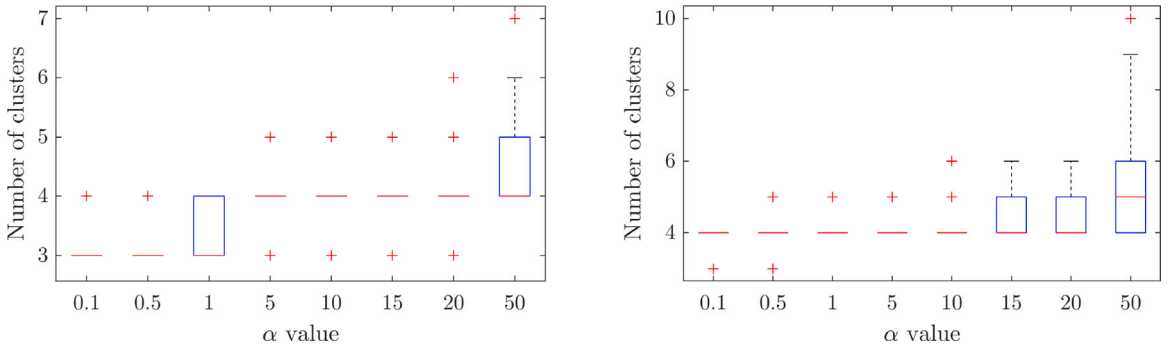

Fig. A.19. The number of clusters formed for a range of α values for two example tools (left — A4 and right — B3). A hundred repeats were conducted for each α value.

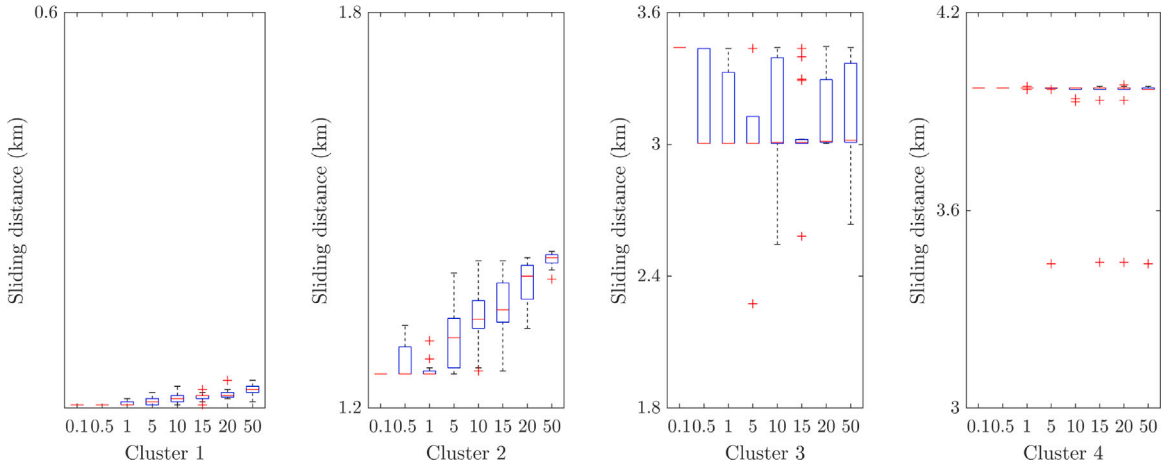

Fig. A.20. The cluster initiations of tool A4 (when four clusters are initiated) according to α.

Declaration of competing interest

The authors declare the following financial interests/personal relationships which may be considered as potential competing interests: Chandula T Wickramarachchi reports financial support, equipment, drugs, or supplies, and travel were provided by Element Six Ltd. Chandula Wickramarachchi reports financial support was provided by Engineering and Physical Sciences Research Council. Chandula Wickramarachchi reports a relationship with Element Six Ltd that includes: funding grants. Chandula Wickramarachchi has patent #GB2106582.8 pending to Element Six (UK) Ltd.

Acknowledgements

Element Six Ltd, UK funded this work and also provided the machine, workpieces and tools used in the experiment. This work was also part funded by the EPSRC, UK grant (EP/I01800X/1). The AMRC also extended help and guidance throughout the experiment. E.J. Cross gratefully acknowledges the support of EPSRC, UK grant EP/S001565/1. For the purpose of open access, the author has applied a Creative Commons Attribution (CC BY) licence to any Author Accepted Manuscript version arising.

Appendix. Effect of hyperparameters

In this paper, the hyperparameter α is fixed *a-priori* at 20; low values of α limits the number of clusters that are initiated. Tuning of the hyperparameter α and threshold values can be used to alter the number of samples in each cluster. However, without knowing the exact nature of the tool when new clusters are initiated, it is difficult/impossible to know which hyperparameters would be optimal. In generic SHM cases, the presence of a crack is treated as damage and cross-validation can be used with false negative rates for checking misclassification of the DPMM, aiding the tuning of hyperparameter, α. If the clusters are well separated, then the number of clusters generated is insensitive to the α parameter [30].

As the DPMM is used in this work to cluster data online, the value of α cannot be learned *a-priori* to find the optimum distribution. To understand the effect of the α parameter, the features used to obtain the result for tools A4 and B3 (in Figs. 12 and 15 respectively)

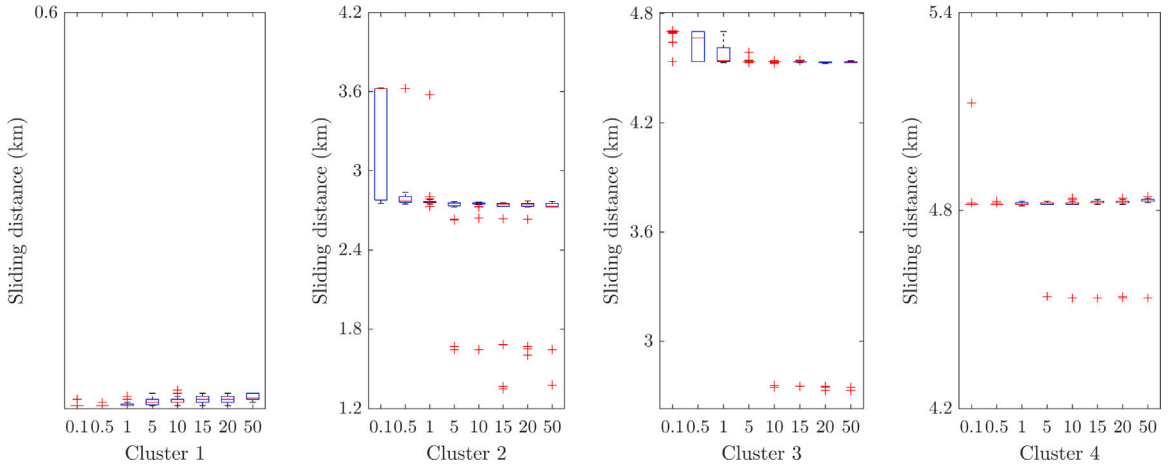

Fig. A.21. The cluster initiations of tool B3 (when four clusters are initiated) according to α.

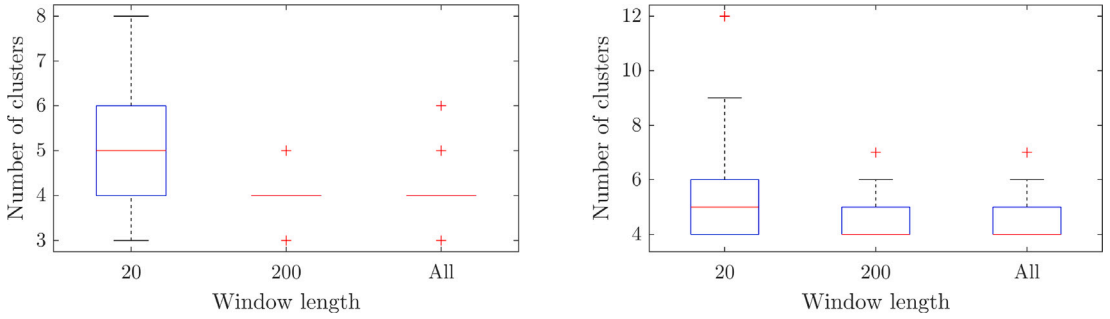

Fig. A.22. The number of clusters formed for window lengths 20, 200 and the entire dataset for tools (A4 — left and B3 — right). Fifty repeats were conducted for each window length.

were fed through the algorithm for a number of α values. In each case, the algorithm was repeated 50 times to obtain the average number of initiated clusters. The results have been presented using a box plot in Fig. A.19. The average number (median) of clusters across the 50 runs are shown with the red line, the outliers are shown in red crosses which stray beyond $\pm 2.7\sigma$ (annotated by the whiskers). The top and the bottom of the boxes represent the 75^{th} and 25^{th} percentiles respectively.

It is clear from Fig. A.19 that the number of clusters are almost independent of the α value when α is small since α only provides a prior over the strength of initiating a new cluster. It is worth considering that this α value, being only a prior hyperparameter, is still subject to the evidence in the data and for well separated clusters (as seen in this work), its effect is, therefore, moderated by the expressive power of the likelihood. When considering α values between 0.1 and 50, the mean number of clusters changes very little. Compared to a traditional periodic inspection regime, choosing α values below 50 provides fewer inspections. The recommendation here, therefore, is that any value of α between 0.1 and 50 can be used without significantly affecting the formation of number of clusters. This is reassuring in the context of TCM as the method is, broadly speaking, insensitive to this user choice.

Figs. A.20 and A.21 show the sliding distances at which the clusters initiate when α is varied for tools A4 and B3 respectively. Again, the median values of sliding distance do not vary significantly with α in the observed range.

The window length of the Gibbs sampler could also affect the results of the DPMM because it is a value that can impact the number of clusters and the points of cluster initiations. This is because the window length governs the number of data points that are re-evaluated by the algorithm. The window length must be sufficiently large to ensure the Markov chain converges into the stationary distribution. Nevertheless, increasing the window length will increase the computational time of the process as larger numbers of datapoints are re-evaluated at each iteration. To investigate the influence of the window length on the DPMM results, data from tools A4 and B3 were evaluated over 50 runs. Fig. A.22 shows the number of clusters initiated by the algorithm when using window lengths of 20 (around 2% of the dataset), 200 (around 20% of the dataset), and a window length that captures the entire tool life (100% or 'All' of the dataset), whist Fig. A.23 shows the corresponding computational times. On average, the number of clusters initiated between a window length of 200 and the entire dataset is consistent, whereas a window length of 20 leads to a larger variance within the number of initiated clusters, suggesting that the Markov chain has not converged to the stationary distribution. Figs. A.24 and A.25 presents the sliding distances at which the clusters initiate for tools A4 and B3 (respectively), when four clusters are initiated (a value of four was chosen here following the 'All' cases in Fig. A.22). Again, the box plots show

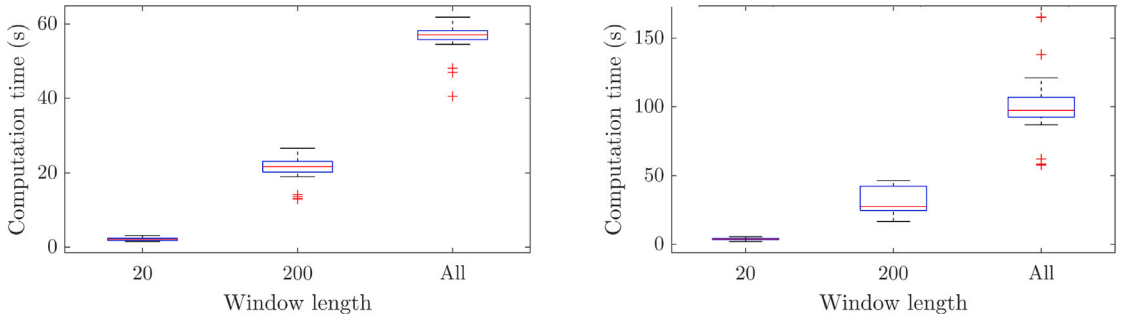

Fig. A.23. The computational time taken for window lengths 20, 200 and the entire dataset for tools (A4 — left and B3 — right).

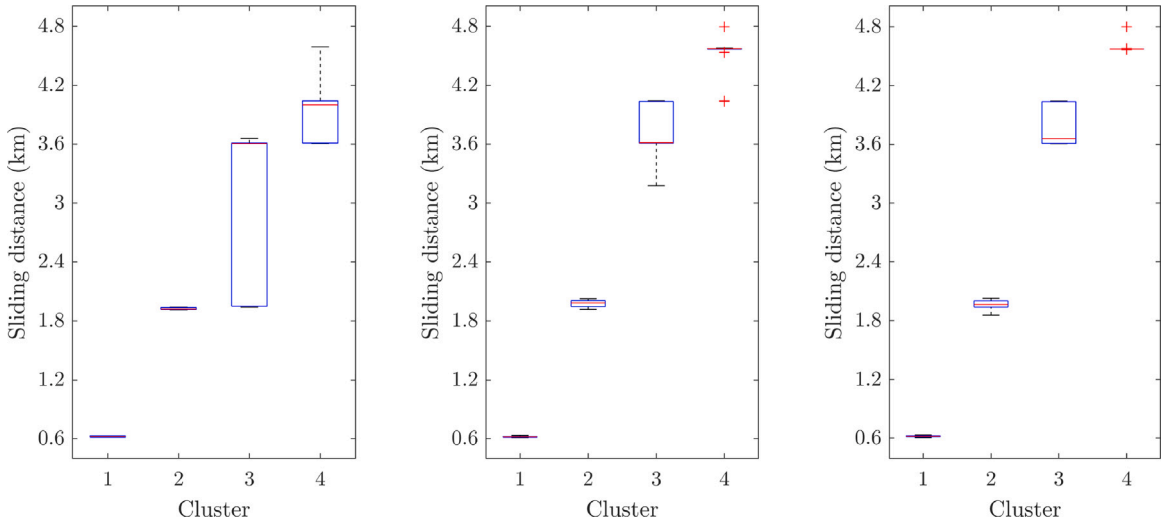

Fig. A.24. The cluster initiations (when four clusters are initiated) for window lengths 20 (left), 200 (middle) and the entire dataset (right) for tool A4.

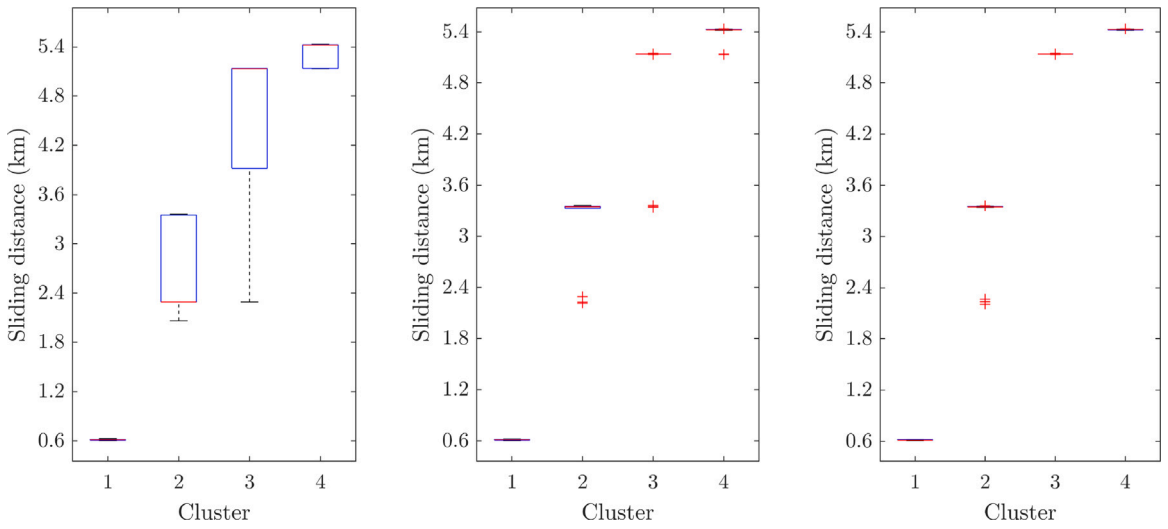

Fig. A.25. The cluster initiations (when four clusters are initiated) for window lengths 20 (left), 200 (middle) and the entire dataset (right) for tool B3.

that a window lengths of 200 and 'All' are similar, whereas the results for the window length of 20 are not. Consequently, a window length of 200 was chosen for this work as it allows the DPMM to performs similarly to the case where the entire dataset is used without the additional computational cost.

References

[1] E. Trent, P. Wright, Metal Cutting, fourth ed., Butterworth-Heinemann, 2000, p. 446.
[2] A. Bhattacharyya, I. Ham, Analysis of tool wear — part I: Theoretical models of flank wear, J. Eng. Ind. 91 (1969) 790–796.
[3] V. Šolaja, Wear of carbide tools and surface finish generated in finish turning of steel, Wear 2 (1958) 40–58.
[4] H. Wiklund, Bayesian and regression approaches to on-line prediction of residual tool life, Qual. Reliab. Eng. Int. 14 (1998) 303–309.
[5] H.V. Ravindra, Y.G. Srinivasa, R. Krishnamurthy, Acoustic emission for tool condition monitoring in metal cutting, Wear 212 (1997) 78–84.
[6] E. Emel, E. Kannatey-Asibu, Acoustic emission and force sensor fusion for monitoring the cutting process, Int. J. Mech. Sci. 31 (1989) 795–809.
[7] S. Dolinšek, J. Kopač, Acoustic emission signals for tool wear identification, Wear 225–229 (1999) 295–303.
[8] A.G. Rehorn, J. Jiang, P.E. Orban, State-of-the-art methods and results in tool condition monitoring: A review, Int. J. Adv. Manuf. Technol. 26 (2005) 693–710.
[9] P.N. Botsaris, J.A. Tsanakas, State-of-the-art in methods applied to tool condition monitoring (TCM) in unmanned machining operations: A review, in: The International Conference of COMADEM, 2008, pp. 73–87.
[10] J.V. Abellan-Nebot, F. Romero Subirón, A review of machining monitoring systems based on artificial intelligence process models, Int. J. Adv. Manuf. Technol. 47 (2010) 237–257.
[11] N. Ambhore, D. Kamble, S. Chinchanikar, V. Wayal, Tool condition monitoring system: A review, Mater. Today: Proc. 2 (2015) 3419–3428.
[12] Y. Zhou, W. Xue, Review of tool condition monitoring methods in milling processes, Int. J. Adv. Manuf. Technol. 96 (2018) 2509–2523.
[13] A. Siddhpura, R. Paurobally, A review of flank wear prediction methods for tool condition monitoring in a turning process, Int. J. Adv. Manuf. Technol. 65 (2013) 371–393.
[14] D.E. Dimla, P.M. Lister, On-line metal cutting tool condition monitoring. II: tool-state classification using multi-layer perceptron neural networks, Int. J. Mach. Tools Manuf. 40 (2000) 769–781.
[15] I. Deiab, K. Assaleh, F. Hammad, On modeling of tool wear using sensor fusion and polynomial classifiers, Mech. Syst. Signal Process. 23 (2009) 1719–1729.
[16] J.S. Kwak, J.B. Song, Trouble diagnosis of the grinding process by using acoustic emission signals, Int. J. Mach. Tools Manuf. 41 (2001) 899–913.
[17] O. Olufayo, K. Abou-El-Hossein, Tool life estimation based on acoustic emission monitoring in end-milling of H13 mould-steel, Int. J. Adv. Manuf. Technol. 81 (2015) 39–51.
[18] K. Worden, E.J. Cross, N. Dervilis, E. Papatheou, I. Antoniadou, Structural health monitoring: from structures to systems-of-systems, IFAC-Papersonline 48 (2015) 1–17.
[19] N. Dervilis, K. Worden, E.J. Cross, On robust regression analysis as a means of exploring environmental and operational conditions for SHM data, J. Sound Vib. 347 (2015) 279–296.
[20] J.H. Zhou, C.K. Pang, Z.W. Zhong, F.L. Lewis, Tool wear monitoring using acoustic emissions by dominant-feature identification, IEEE Trans. Instrum. Meas. 60 (2011) 547–559.
[21] T.E. Mcleay, Unsupervised monitoring of machining processes, (Ph.D. thesis), University of Sheffield, 2016.
[22] E. Ramasso, V. Placet, R. Gouriveau, L. Boubakar, N. Zerhouni, Health assessment of composite structures in unconstrained environments using partially supervised pattern recognition tools, in: Annual Conference of the PHM Society, Vol. 4, 2012.
[23] E. Ramasso, V. Placet, M.L. Boubakar, Unsupervised consensus clustering of acoustic emission time-series for robust damage sequence estimation in composites, IEEE Trans. Instrum. Meas. 64 (2015) 3297–3307.
[24] P. Angelov, D.P. Filev, N. Kasabov, Evolving Intelligent Systems: Methodology and Applications, John Wiley & Sons, 2010.
[25] D.D. Doan, E. Ramasso, V. Placet, S. Zhang, L. Boubakar, N. Zerhouni, An unsupervised pattern recognition approach for AE data originating from fatigue tests on polymer–composite materials, Mech. Syst. Signal Process. 64 (2015) 465–478.
[26] K. Javed, R. Gouriveau, N. Zerhouni, A new multivariate approach for prognostics based on extreme learning machine and fuzzy clustering, IEEE Trans. Cybern. 45 (2015) 2626–2639.
[27] A. Vlachos, A. Korhonen, Z. Ghahramani, Unsupervised and constrained Dirichlet process mixture models for verb clustering, in: GEMS '09 Proceedings of the Workshop on Geometrical Models of Natural Language Semantics, 2009, pp. 74–82.
[28] M. Dreyer, J. Eisner, Discovering morphological paradigms from plain text using a Dirichlet process mixture model, in: Proceedings of the 2011 Conference on Empirical Methods in Natural Language Processing, 2011, pp. 616–627.
[29] A.R.F. da Silva, A Dirichlet process mixture model for brain MRI tissue classification, Med. Image Anal. 11 (2007) 169–182.
[30] T.J. Rogers, K. Worden, R. Fuentes, N. Dervilis, U.T. Tygesen, E.J. Cross, A Bayesian non-parametric clustering approach for semi-supervised structural health monitoring, Mech. Syst. Signal Process. 119 (2019) 100–119.
[31] S. Liang, J. Yu, D. Tang, H. Liu, A Bayesian nonparametric approach for tool condition monitoring, in: 2016 UKACC 11th International Conference on Control (CONTROL), IEEE, 2016, pp. 1–6.
[32] C.E. Rasmussen, The infinite Gaussian mixture model, in: Advances in Neural Information Processing Systems 12, 2000, pp. 554–560.
[33] C.E. Rasmussen, Z. Ghahramani, Infinite mixtures of Gaussian process experts, in: Advances in Neural Information Processing Systems, Vol. 14, 2001, pp. 881–888.
[34] T.J. Rogers, A Bayesian non-parametric clustering approach for semi-supervised structural health monitoring, 119, 2019.
[35] Physical Acoustics Corporation, Micro30D sensor, 2013, https://www.physicalacoustics.com/content/literature/sensors/Model_Micro30D.pdf, Accessed:8-10-2021.
[36] D.A. Dornfeld, Y. Lee, A. Chang, Monitoring of ultraprecision machining processes, Int. J. Adv. Manuf. Technol. 21 (2003) 571–578.
[37] C.T. Wickramarachchi, T.E. McLeay, S. Ayvar-Soberanis, W. Leahy, E.J. Cross, Tool wear inspection of polycrystalline cubic boron nitride inserts, in: Special Topics in Structural Dynamics, Vol. 5, 2019, pp. 259–266.
[38] W. Dai, J. Sun, Y. Chi, Z. Lu, D. Xu, N. Jiang, Review of machining equipment reliability analysis methods based on condition monitoring technology, Appl. Sci. 9 (2019) 2786.
[39] M. Prakash, M. Kanthababu, A.A.J. Kumar, N. Arun, V.P. Venkadesan, Identification of tool wear status and correlation of chip morphology in micro-end milling of mild steel (SAE 1017) using acoustic emission signal, in: IOP Conference Series: Materials Science and Engineering, Vol. 912, 2020, 032066.
[40] B. Wang, Z. Liu, Acoustic emission signal analysis during chip formation process in high speed machining of 7050-T7451 aluminum alloy and Inconel 718 superalloy, J. Manuf. Process. 27 (2017) 114–125.
[41] X. Li, A brief review: Acoustic emission method for tool wear monitoring during turning, Int. J. Mach. Tools Manuf. 42 (2002) 157–165.
[42] D.-E. Lee, I. Hwang, C.M. Valente, J.F.G. Oliveira, D.A. Dornfeld, Precision manufacturing process monitoring with acoustic emission, in: Condition Monitoring and Control for Intelligent Manufacturing, Springer, 2006, pp. 33–54.
[43] J. Bhaskaran, M. Murugan, N. Balashanmugam, M. Chellamalai, Monitoring of hard turning using acoustic emission signal, J. Mech. Sci. Technol. 26 (2012) 609–615.
[44] J.H. Cantrell, Substructural organization, dislocation plasticity and harmonic generation in cyclically stressed wavy slip metals, Proc. R. Soc. Lond. A. A Math. Phys. Eng. Sci. 460 (2004) 757–780.
[45] C.T. Wickramarachchi, Automated testing of advanced cutting tool materials, (Ph.D. thesis), University of Sheffield, 2019.
[46] H. Sohn, Effects of environmental and operational variability on structural health monitoring, Phil. Trans. R. Soc. A 365 (2007) 539–560.

[47] E.J. Cross, K. Worden, Q. Chen, Cointegration: A novel approach for the removal of environmental trends in structural health monitoring data, Proc. R. Soc. Lond. A. Math. Phys. Eng. Sci. 467 (2011) 2712–2732.
[48] E.J. Cross, G. Manson, K. Worden, S.G. Pierce, Features for damage detection with insensitivity to environmental and operational variations, Proc. R. Soc. Lond. A. Math. Phys. Eng. Sci. 468 (2012) 4098–4122.
[49] N. Dervilis, R.J. Barthorpe, I. Antoniadou, W.J. Staszewski, K. Worden, Damage detection in carbon composite material typical of wind turbine blades using auto-associative neural networks, in: Health Monitoring of Structural and Biological Systems 2012, 2012, pp. 61–72.
[50] N. Dervilis, E.J. Cross, R.J. Barthorpe, K. Worden, Robust methods of inclusive outlier analysis for structural health monitoring, J. Sound Vib. 333 (2014) 5181–5195.